ISSN 0030-400X, Optics and Spectroscopy, 2015, Vol. 118, No. 1, pp. 37–45. © Pleiades Publishing, Ltd., 2015.
Original Russian Text © O.K. Bazyl, V.A. Svetlichnyi, 2015, published in Optika i Spektroskopiya, 2015, Vol. 118, No. 1, pp. 40–49.

CONDENSED-MATTER SPECTROSCOPY

# Features of the Electronic Structure and Photophysical Processes in Asymmetric and Symmetric (Dicyanomethylene)-pyran Dyes

**O. K. Bazyl and V. A. Svetlichnyi**

*Siberian Physical Technical Institute of Tomsk State University, Tomsk, 634050 Russia*

*e-mail: okbazyl@rambler.ru*

Received June 4, 2014

**Abstract**—The electronic structure and photophysical processes in (dicyanomethylene)-pyran dyes, DCM and bis-DCM, have been studied by methods of quantum chemistry and optical spectroscopy. The spectral-luminescence and proton-acceptor properties for *trans* and *cis* conformers are investigated theoretically. The influence of the pyran ring geometry on the aforementioned properties and the efficiency of intramolecular photophysical processes in these molecules are analyzed. Simulation of *trans–cis* photoisomerization is performed, and its influence on the spectral-luminescence properties is studied.

**DOI:** 10.1134/S0030400X1501004X

## INTRODUCTION

Merocyanine dye 4-(dicyanomethylene)-2-methyl-6[*para*-(dimethylamino)styryl]-4H-pyran (DCM) is a well-known fluorophor, which is used in tunable lasers, nonlinear optics, electroluminescent devices, and solar cells [1–4]. Due to the large Stokes shift, which leads to a weak overlap of the absorption and fluorescence spectra and, therefore, to a small loss on reabsorption, DCM dye is efficient for light converters, including luminescent solar concentrators [5, 6]. The DCM molecule is an important basis for a number of new high-efficiency dyes used in optical technologies [7–10].

A characteristic feature of DCM, which determines its functional properties, is the simultaneous presence of donor and acceptor groups in the dye molecule, which are interconnected by an unsaturated bridge bond (Fig. 1a). This configuration leads to a significant separation of unlike charges even in the ground state, a separation that becomes even more pronounced in the excited state. The charge separation in the DCM molecule ensures its significant dipole moment in both the ground and excited electronic states and determines its electrical properties [3, 8]. For the same reason, the position of the absorption and fluorescence bands depends on the solvent polarity.

The optical properties and photoprocesses in the DCM molecule and its derivatives are of great interest for researchers [5, 11–20]. The radiative and nonradiative decay of the fluorescent state of DCM and its substituted and the influence of the solvent properties, temperature, and structure of donor and acceptor fragments on the photophysical processes in dye molecules have been experimentally studied in [5, 11–14, 17, 20]. In particular, the *trans–cis* photoisomerization was considered. This reaction may have a significant quantum yield in nonpolar solvents, which results in simultaneous presence of *trans* and *cis* isomers in

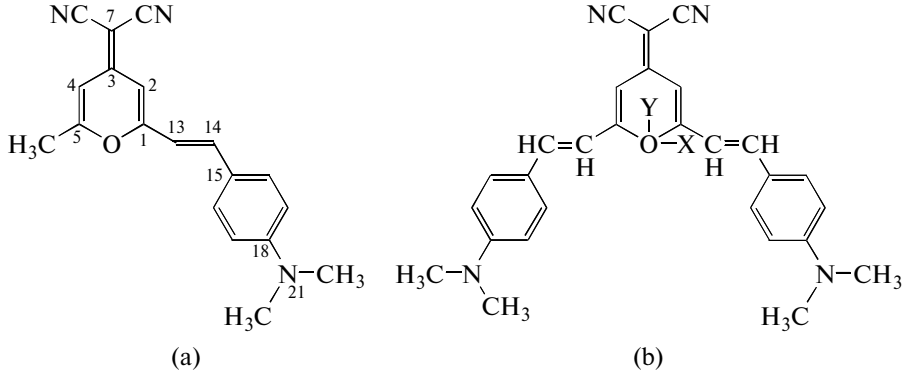


**Fig. 1.** Structural formulas of (a) DCM and (b) bis-DCM *trans* isomers.

the medium [5, 11]. The presence of groups with opposite donor–acceptor properties at different sides of the ethylene fragment in the DCM molecule makes the double character of the ethylene bond less pronounced, thus facilitating rotation around it. This is confirmed by the results of optimization of the DCM-molecule geometry in the ground and excited states, which indicate alignment of the lengths of C–C bonds in the ethylene fragment to a one-and-a-half length in the ground state [21]. Molecules of this series have been investigated in [15, 16, 18, 19] by methods of quantum chemistry. The spectra and rate constants of the photophysical processes responsible for the decay of fluorescent state $S_1$ in an isolated DCM molecule were calculated in [18] by the method of intermediate neglect of differential overlap (INDO) with spectroscopic parameterization [22]. The results of calculation showed that, with photoisomerization disregarded, the fluorescence in an isolated molecule competes with internal and singlet–triplet conversions. The ratio of the rate constants of radiative and nonradiative processes in DCM ($k_r = 2 \times 10^8 > k_{IC} = 10^8 > k_{(S_1 \to T_3)} = 10^7\ s^{-1}$) yields calculated quantum fluorescence yield $\Phi_{fl} = 0.6$, which corresponds to the experimental values for polar solvents [17]. The results of studying the spectrum of DCM molecule by other semiempirical [19] and ab initio methods [15, 16], in contrast to the data of [18], differ significantly from the experimental results in both the energies and/or oscillator strengths of the electron transitions responsible for the absorption bands; this discrepancy indicates the complexity of the problem stated. Note that the calculations in all the aforementioned studies were performed for only *trans* isomers with one pyran-cycle conformation; the proton-acceptor properties of DCM were not investigated to a full extent. It should be noted that the symmetrically substituted bis-DCM molecule (Fig. 1b) [18, 14] and its derivatives have been analyzed much less thoroughly.

In this paper, we report the results of studying the specific features of electronic structure, the efficiency of photophysical processes, and the proton-acceptor properties of *trans* and *cis* isomers of merocyanine DCM and bis-DCM dyes for two pyran-cycle configurations ("boat" and "chair") by methods of quantum chemistry. This study is urgent because there is a need for a unified approach, within which one could not only interpret electronic spectra and calculate constants of intramolecular photophysical processes, but also consider the process of intramolecular charge transfer and estimate the proton-acceptor properties of the ground and excited electronic states of the dye molecules. These data are important for practical use of merocyanine dyes in optoelectronics.

## OBJECTS AND METHODS OF STUDY

DCM and bis-DCM dyes were synthesized by Ponomareva (OOO NPF Deltakor); their structure was confirmed by standard methods of NMR spectroscopy. The purity of dyes was controlled by thin-layer chromatography. A DCM dye produced by Radiant Dyes Chemie was also used for comparison.

The spectra of absorption, fluorescence, and fluorescence excitation anisotropy (polarization spectra) [23] were recorded with an SM2203 spectrofluorimeter (ZAO SOLAR) and Cary 100 spectrophotometer (Varian).

Quantum-chemical calculations of the spectra and rate constants of intramolecular photophysical processes of fluorescent state decay were performed by the semiempirical INDO method with parameterization [22]. When choosing the molecular geometry, we used averaged bond lengths and bond angles in accordance with [24] and optimized the molecular structure. The optimization showed that the pyran cycle has an out-of-plane structure. Calculations were performed for the following configuration: carbon atoms 1, 2, 4, and 5 of the pyran cycle (Fig. 1) are removed from the molecular plane by $Z = -0.2$ Å, $C_3$ atoms are removed by $Z = 0.2$ Å, and $O_6$ atoms are removed by $Z = 0.2$ Å (boat conformation) or $-0.6$ Å (chair conformation). For these values of $Z$ coordinates, the bond lengths are identical in both conformations of the pyran cycle of *trans* and *cis* isomers. When calculating *cis* isomers in sterically unstrained molecular structures, the angle between the planes of pyran and phenyl (along with the dimethylamino group) fragments was taken to be 70°. Although the Stokes shift of the fluorescence band for the molecules under study does not exceed 3000 $cm^{-1}$, the fluorescence spectrum was calculated with allowance for the change in the bond lengths by calculating the bond occupancies in the ground and excited states according to Mulliken [25].

## RESULTS AND DISCUSSION

### *Nature of Electronic States and Absorption Spectra*

According to the calculations, the long-wavelength absorption band of *trans* isomers of DCM and bis-DCM is due to the $S_0 \to S_1(\pi\pi^*)$ transition, which is polarized along the short molecular axis. The $S_0 \to S_2(\pi\pi^*)$ transition is less intense and only slightly pronounced in the absorption spectrum against the background of the first strong transition. However, since it is polarized perpendicular to the $S_0 \to S_1(\pi\pi^*)$ transition, it can be distinguished well in the fluorescence anisotropy spectra. A similar situation is observed for other high-lying transitions with polarizations different from that of the $S_0 \to S_1(\pi\pi^*)$ transition (Table 1). Thus, the absorption in the range up to 33000 $cm^{-1}$ forms several more electronic transitions of the $\pi\pi^*$ type with different polarizations.

**Table 1.** Energies $E_n$, oscillator strengths $f$, and polarizations $P$ of the $S_0 \longrightarrow S_n$ transitions for different conformations of DCM and bis-DCM* molecules

| Calculation | | | | | | | | Experiment | | | |
|---|---|---|---|---|---|---|---|---|---|---|---|
| boat | | | | chair | | | | *n*-hexane | petrolatum | | ethyl acetate |
| | | | | | | | | absorption | absorption | polarization | absorption |
| $S_n$ | $E_n$, $cm^{-1}$ | $f$ | $P$ | $S_n$ | $E_n$, $cm^{-1}$ | $f$ | $P$ | $S_n$ | | | |
| DCM *trans* isomer | | | | | | | | | | | |
| 1 | 21320 | 0.682 | $Y$ | 1 | 21612 | 0.532 | $Y$ | 22000 | 21800 | | 22000 |
| 2 | 26120 | 0.134 | $X$ | 2 | 25380 | 0.259 | $X$ | | | 25600 | |
| 3 | 28430 | 0.253 | $X$ | 3 | 29410 | 0.188 | $X$ | | | 27500 | |
| 4 | 31760 | 0.450 | $Y$ | 4 | 32260 | 0.354 | $Y$ | | | | |
| 6 | 32800 | 0.070 | $X$ | 6 | 32840 | 0.126 | $X$, $Y$ | | | 33000 | |
| DCM *cis* isomer | | | | | | | | | | | |
| 1 | 22470 | 0.561 | $X$ | 1 | 22650 | 0.497 | $X$ | 22000 | 21800 | | 22000 |
| 4 | 30830 | 0.052 | $Y$ | 4 | 32090 | 0.084 | $Z$ | | | 25600 | |
| 5 | 32150 | 0.077 | $X$, $Z$ | 5 | 32740 | 0.064 | $X$ | | | 27500 | |
| 6 | 32830 | 0.061 | $Y$ | 6 | 32800 | 0.172 | $X$, $Y$ | | | 33000 | |
| bis-DCM *trans* isomer | | | | | | | | | | | |
| 1 | 21550 | 0.770 | $Y$ | 1 | 21250 | 0.678 | $Y$ | 22200 | 21600 | | 21000 |
| 2 | 24270 | 0.570 | $X$ | 2 | 24900 | 0.570 | $X$ | | | 25000 | |
| 3 | 27500 | 0.117 | $X$ | 3 | 27980 | 0.114 | $X$ | | | 28000 | |
| 4 | 30940 | 0.676 | $Y$ | 4 | 31080 | 0.767 | $Y$ | | | | |
| 8 | 33060 | 0.423 | $X$ | 8 | 33020 | 0.161 | $X$ | | | 33000 | |
| bis-DCM *cis* isomer | | | | | | | | | | | |
| 1 | 22640 | 0.379 | $Y$ | 1 | 21780 | 0.306 | $Y$ | 22200 | 21600 | | 21000 |
| 2 | 26190 | 0.233 | $X$ | 2 | 22620 | 0.211 | $X$, $Y$ | | | 25000 | |
| 3 | 28640 | 0.155 | $X$ | 3 | 29270 | 0.212 | $X$ | | | 28000 | |
| 7 | 32940 | 0.114 | $Z$ | 8 | 33080 | 0.116 | $Z$ | | | 33000 | |

* The table contains characteristics of electronic transitions of the $\pi\pi^*$ type, which are responsible for bands in the experimental absorption spectra of DCM and bis-DCM.

A comparison of the calculation results for *trans* isomers of DCM and bis-DCM with different pyran-cycle configurations (boat or chair) shows that both conformations yield electronic transitions with close energies and intensities and characterized by similar polarizations; they have no fundamental differences in the formation of absorption spectrum in the visible and near-UV spectral region (Table 1).

A comparative analysis of the experimental spectra, orbital nature of electronic excited states (Table 1), and localization of the molecular orbitals forming the $S_1(\pi\pi^*)$ states (Fig. 2) of the molecules of *trans* isomers of DCM and bis-DCM showed the similarity of the electronic transitions in these molecules. The introduction of the second donor group into the *trans* isomer of DCM (i.e., transition to bis-DCM) is accompanied by a small blue shift of the band peaks in the experimental absorption spectra (Table 1) and calculated electronic transitions responsible for these absorption bands. As was noted above, the geometries of *cis* and *trans* isomers are significantly different: the pyran and substituent (phenyl ring with a dimethyl amino group) planes form an angle of 70° in sterically unstrained *cis* isomers. This circumstance significantly violates the $\pi$ conjugation between the aromatic fragments of the molecule and, as consequence, leads to a blue shift of absorption bands and reduction of their intensity. However, calculations showed that these variations in the energy and intensity of electronic transitions in the *cis* and *trans* isomers of DCM and bis-DCM molecules are small (Table 1). The electronic transitions in isomers are also similar in the localization of the molecular orbitals forming them; some differences in the polarizations of the electronic transitions in *trans* and *cis* isomers are explained by changes in the spatial position of molecular fragments

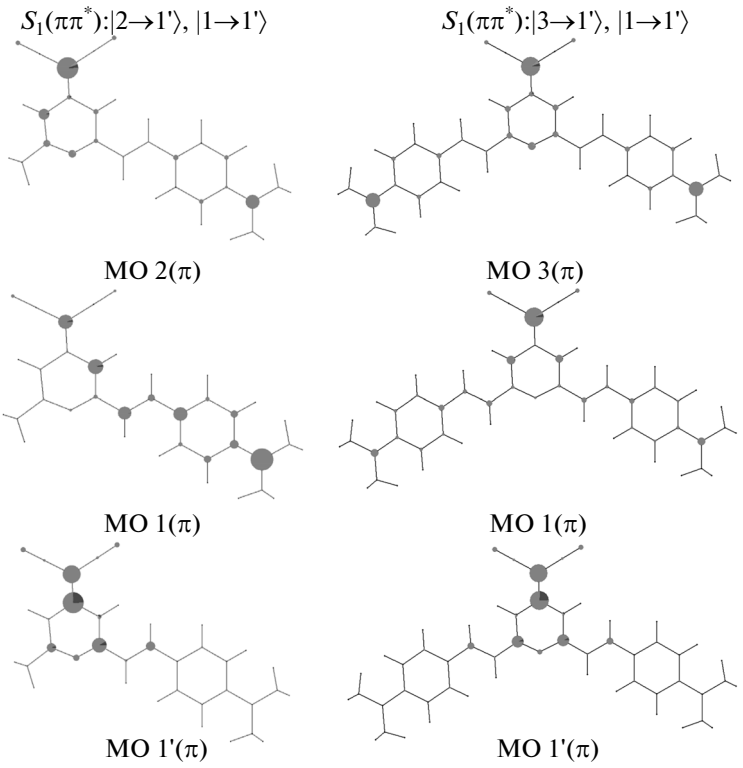


**Fig. 2.** Localization of molecular orbitals (MOs) involved in the formation of the $S_1(\pi\pi^*)$ state of *trans* isomers of DCM and bis-DCM molecules.

(between which electron density is transferred) with respect to each other.

Thus, since the transition from *trans* to *cis* isomers in both molecules is accompanied by a very small spectral shift within the long-wavelength absorption band, their spectra can hardly be experimentally distinguished.

The calculated dipole moment of the *trans* isomer of DCM molecule in the ground state is 10.3D; this value is close to the experimental result (10.2D) obtained in [10] and the calculation results of [15, 16]. This confirms the correctness of the calculation of electron-density distribution in the DCM molecule by the INDO method with parameterization [22]. In the $S_1(\pi\pi^*)$ state, the dipole moment increases to 12.5D. An increase in the dipole moment in the $S_1$ state was also noted in [11]; however, its absolute values were inconsistent with our results and the data of [10, 15, 16]. Our calculations yield an excitation-induced increase in the dipole moment close to that reported in [11] (to 20D) for only some electronic excited states of DCM, which provide absorption in the range to 33000 $cm^{-1}$, in the DCM conformation with a dimethylamino group, deviated from the molecular plane by 90°.

To the best of our knowledge, there are no experimental data on the dipole moment values for the bis-DCM molecule. The calculated values of the dipole moment of bis-DCM in the ground (11.2D) and excited singlet (12.9D) states of this molecule are close to the corresponding data for DCM.

### *Fluorescence and Photophysical Processes in Molecules*

Experimental studies of dye molecules in solutions show that the quantum fluorescence yield of DCM depends strongly on the solvent properties: it changes from 0.005 in hexane to 0.5–0.9 in polar solvents [17]. The bis-DCM molecule fluoresces worse: $\Phi_{fl}$ does not exceed 0.1 in ethyl acetate and ethanol solvents [26]. The quantum yield of bis-DCM decreases in both highly polar ($\Phi_{fl} = 0.01$ in dimethyl sulfoxide) and nonpolar ($\Phi_{fl} = 0.004$ in hexane) solvents. As far as we know, there are no experimental data on these dyes in the gas phase, where individual properties of isolated molecules could be observed.

Comparison of the calculation results for isolated molecules with the experimental data for nonpolar hexane and weakly polar solvents (e.g., ethyl acetate) (Table 2) shows good correspondence in fluorescence energies for both *trans* and *cis* isomers of DCM and bis-DCM, independent of the pyran-cycle geometry (boat or chair). The *trans* isomers of DCM and bis-DCM molecules describe well the fluorescence and

**Table 2.** Energies of $S_1 \longrightarrow S_0$ transitions and fluorescence quantum yields for different conformations of DCM and bis-DCM isomers

| Molecule geometry | | Calculation | | Experiment | | | |
|---|---|---|---|---|---|---|---|
| isomer | pyran cycle | $E_{fl}$, $cm^{-1}$ | $\Phi_{fl}$ | *n*-hexane | | ethyl acetate [18] | |
| | | | | $E_{fl}$, $cm^{-1}$ | $\Phi_{fl}$ | $E_{fl}$, $cm^{-1}$ | $\Phi_{fl}$ |
| DCM | | | | | | | |
| *Trans* | boat | 20140 | 0.42 | 20200 | 0.005 | 18690 | 0.5 |
| | chair | 20240 | 0.49 | | | | |
| *Cis* | boat | 18290 | 0.17 | | | | |
| | chair | 19170 | 0.05 | | | | |
| bis-DCM | | | | | | | |
| *Trans* | boat | 20390 | 0.20 | 20700 | 0.004 | 18320 | 0.1 |
| | chair | 20400 | 0.16 | | | | |
| *Cis* | boat | 16570 | 0.03 | | | | |
| | chair | 17050 | 0.04 | | | | |

quantum fluorescence yield in low-polarity solvents (ethyl acetate).

Calculations for isolated molecules show that photophysical processes in *trans* isomers of both molecules have no fundamental differences in dependence of the pyran-fragment geometry (chair or boat). Radiative decay constant $k_r$ is about $2 \times 10^8\ s^{-1}$, which is more than an order of magnitude larger than the constant rate of internal singlet–singlet conversion, while the quantum yield depends on the position of the $S_1(\pi\pi^*)$ state and the nearest triplet states, which determine the intersystem crossing.

Radiative decay rate constant $k_r$ in *cis* conformers decreases insignificantly because of the nonplanar structure of the molecules and violation of the $\pi$ conjugation between the aromatic fragments; at the same time, the internal conversion rate constant increases significantly, which generally leads to a considerable decrease in the fluorescence quantum yield of *cis* isomers, especially for bis-DCM with respect to DCM.

Figure 3 schematically presents the energy-level diagrams and photophysical processes occurring in *trans* and *cis* isomers of the molecules under study in the boat and chair pyran-cycle conformations, which, as was noted above, describe well the spectral-luminescence properties of the dye molecules in low-polarity solvents and are close to the results obtained in [18].

We should note that, despite the fairly large intersystem-conversion rate constant obtained in the calculations for isolated molecules, the experimental data indicate that the channel singlet-triplet conversion does not dominate in the decay of excited DCM states. In particular, a study of the absorption spectra from the excited states of this molecule in methanol demonstrates that the $T_1 \rightarrow T_m$ absorption band arises only in the presence of sensitizer, which facilitates efficient occupation of the $T_1$ state [11, 17].

It is known that, along with the internal conversion, there are efficient decay channels for excited nonrigid molecules (stilbenes, merocyanines, polymethines) in media characterized by weak interaction with solvent (nonpolar and low-polarity solvents) are *trans–cis* isomerization [11, 27] and the possibility of existence of "twisted" nonplanar configurations in the excited state (the so-called TICT states) [28]. As a result of *trans–cis* isomerization, rotation of molecular fragments with respect to each other causes a significant decrease in the energy of the $S_1$ state, as a result of which the efficiency of deexcitation of the excitation energy in the internal conversion channel $S_1 \rightarrow S_0$ increases by several orders of magnitude, whereas the change in the efficiency of other intramolecular processes is much smaller. The possibility of rotating molecular fragments with efficient intramolecular energy transfer in the presence of single or double bonds in their structure (around which this rotation may occur) was also indicated in [21, 29].

To confirm theoretically the possibility of *trans–cis* isomerization of DCM and bis-DCM molecules, we determined (using the INDO method) the most likely molecular bonds in the ethylene chain that allow for this possibility and performed a step-by-step calculation of the photophysical processes in the molecule at different stages of rotation.

The calculation of the occupancy of ethylene-chain bonds in DCM in the ground and fluorescent states showed that rotation in the $S_1$ state changes the occupancy (strength) of single and double bonds, as a result of which rotation of DCM fragments with respect to the double bond is facilitated, while rotation with respect to single bonds is hindered in the $S_1$ state.

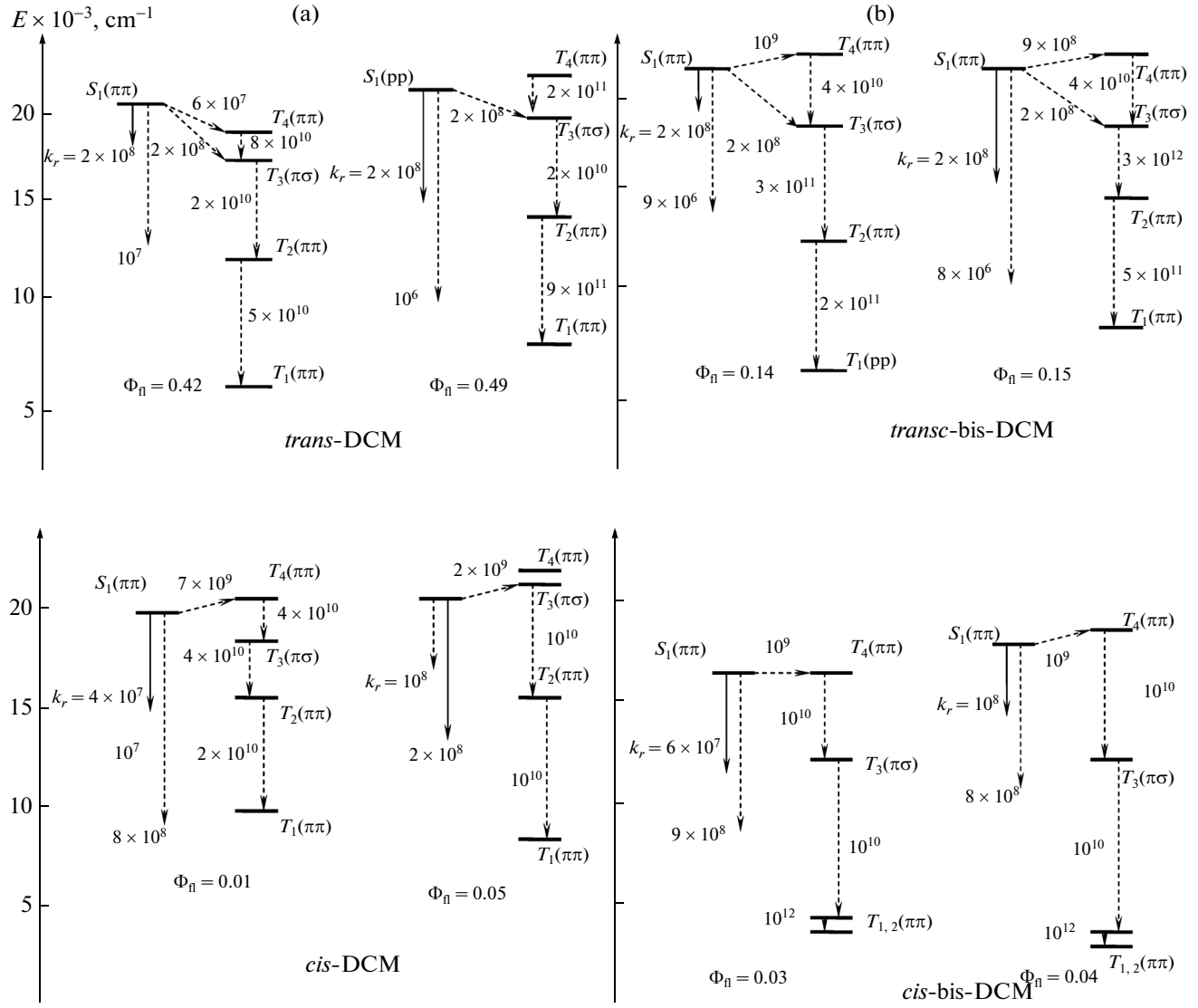


**Fig. 3.** Energy-level diagrams of photophysical processes in *trans* and *cis* isomers of the (a) DCM and (b) bis-DCM molecules with pyran-cycle conformations of the boat (on the left) and chair (on the right) types.

Thus, rotations with respect to specifically double bonds in the ethylene chain are most likely in the fluorescent state. It is noteworthy that largest decrease in occupancy in the fluorescent state is observed for the double C=C bond, which connects the cyano group with the pyran cycle (Table 3); this observation is indicative of possible rotation of the cyano group in the fluorescent state. However, this fact calls for a separate study.

Table 4 contains calculated rate constants for intramolecular photophysical processes at different fixed angles φ between the planes of pyran and phenyl cycles in DCM. These data indicate that the fluorescence quantum yield depends of angle φ between the planes of the aforementioned molecular fragments: it decreases with an increase in φ. The sharpest decrease in $\Phi_{fl}$ occurs at φ values close to 90°. The main reason for the decrease in the fluorescence quantum yield is the increase in the internal conversion rate in the $S_1 \rightarrow S_0$ channel by several orders of magnitude as a result of the significant reduction of the energy of the $S_1$ state. A similar state of affairs is observed for the bis-DCM molecule.

Another likely reason for the decrease in the fluorescence quantum yield of merocyanine and polymethine dyes, especially those having an extended ethylene chain (on which electronic-vibrational transitions from lower excited states are localized), is enhancement of the internal conversion upon interaction with solvent molecules. However, this influence cannot be determined within our theoretical approach.

**Table 3.** Occupancy of some chemical bonds in DCM and its change upon excitation

| State | Chemical bond* | | | | |
|---|---|---|---|---|---|
| | $C_1$–$C_{13}$ | $C_{13}$–$C_{14}$ | $C_{14}$–$C_{15}$ | $C_{18}$–$C_{21}$ | $C_3$–$C_7$ |
| $S_0$ | 0.706 | 1.027 | 0.818 | 0.835 | 0.928 |
| $S_1$ | 0.712 | 0.986 | 0.836 | 0.860 | 0.767 |
| $\Delta p = [p(S_1) - p(S_0)]$, e | Change in bond occupancy | | | | |
| | +0.006 | −0.041 | +0.018 | +0.025 | −0.162 |

* Enumeration of atoms is as in Fig. 1a.

**Table 4.** Energies of the $S_1 \longrightarrow S_0$ transition, rate constants $k$ of photophysical processes, and fluorescence quantum yields $\Phi_{fl}$ in the DCM molecule for different angles φ between the planes of pyran and dimethylamino phenyl fragments

| Parameter | φ, deg | | | | |
|---|---|---|---|---|---|
| | 0 | 30 | 60 | 75 | 90 |
| $E(S_1 \longrightarrow S_0)$, $cm^{-1}$ | 20140 | 20000 | 18490 | 15390 | 9050 |
| $k_r(S_1 \longrightarrow S_0)$, $s^{-1}$ | $2 \times 10^8$ | $3 \times 10^8$ | $3 \times 10^8$ | $1 \times 10^8$ | $2 \times 10^7$ |
| $k_{IC}(S_1 \longrightarrow S_0)$, $s^{-1}$ | $4 \times 10^5$ | $5 \times 10^6$ | $7 \times 10^7$ | $9 \times 10^8$ | $6 \times 10^{10}$ |
| $k_{ic}(S_1 \longrightarrow T_n)$, $s^{-1}$ | $8 \times 10^8$ | $2 \times 10^9$ | $5 \times 10^9$ | $4 \times 10^9$ | $1 \times 10^9$ |
| $\Phi_{fl}$ | 0.20 | 0.12 | 0.05 | 0.03 | $3 \times 10^{-4}$ |

*Electron-Density Distribution and Proton-Acceptor Properties*

Table 5 contains the charge characteristics of individual fragments of the molecules under study with different spatial structures and their change upon excitation to the $S_1(\pi\pi^*)$ state.

In the ground state, fragments of the *trans* and *cis* isomers of DCM molecule exhibit identical properties independently of the chosen pyran-cycle conformation: the pyran cycle, phenyl, and (to a smaller extent) ethylene bridge have donor properties, while cyano groups $C(CN)_2$ exhibit acceptor properties. In fact, the dimethylamino group in the ground state is not involved in the electron-density redistribution between the fragments; it possesses weak acceptor properties in the DCM molecule (Table 5).

In the $S_1(\pi\pi^*)$ state, the pyran cycle of the DCM molecule, independently of its conformation and isomer type, becomes an acceptor due to the enhancement of the donor properties of the phenyl and dimethylamino groups. The degree of charge separation between the donor and acceptor fragments in DCM *cis* isomers is higher than in *trans* isomers. The difference between the pyran-cycle conformations in *cis* isomers affect the change in the fragment electron density in the $S_1(\pi\pi^*)$ state: the charge variation for the pyran cycle and $C(CN)_2$ group in the chair conformation is larger than in the boat conformation.

The pyran cycle, phenyl fragments, and ethylene bridges in the bis-DCM molecule exhibit the same donor–acceptor properties as the corresponding fragments in DCM. The dimethylamino and cyano groups are exceptions: they have weak donor properties in the ground state of the boat conformation of *cis* isomer (Table 5), and their acceptor properties weaken upon excitation.

The electron-density distribution in the ground and excited states yields information on the donor–acceptor properties of individual molecular fragments. However, these data are insufficient for simulating peculiar intermolecular interactions between the molecule under study and molecules of the proton-donor solvent, because a center with a high electron density can be surrounded by atoms or molecular fragments having a positive charge and screening this center. Additional information on the proton-acceptor properties of molecule can be derived from the molecular electrostatic potential (MEP), which describes the interaction energy of a spatially distributed molecular charge with a positive test charge at a chosen point in the space around the molecule. The calculated MEP values for isomers of investigated molecules with different pyran-cycle conformations are listed in Table 6. Analysis of the MEP showed that nitrogen atoms of the cyano group and oxygen of the pyran cycle are responsible (to different extents) for the proton-acceptor properties in the ground and excited states of both molecules. The nitrogen atom of the dimethylamino group, being located near carbon atoms with effective positive charges, does not provide an MEP minimum, despite effective negative charge $q_N = -0.262\ e$ and $q_N = -0.244\ e$ in the ground and excited states, respectively. In the excited state, the MEP value

**Table 5.** Electron density ($q$) and its change ($\Delta q$) upon electronic excitation of fragments of DCM and bis-DCM molecules for different conformations

| Fragment | $q(S_0)$, $e$ | $q(S_1)$, $e$ | $\Delta q(S_1)$, $e$ | $q(S_0)$, $e$ | $q(S_1)$, $e$ | $\Delta q(S_1)$, $e$ |
|---|---|---|---|---|---|---|
| | boat | | | chair | | |
| *trans*-DCM | | | | | | |
| Pyran cycle | 0.191 | −0.077 | 0.268 | 0.159 | −0.078 | 0.237 |
| $C(CN)_2$ | −0.270 | −0.362 | 0.092 | −0.252 | −0.378 | 0.126 |
| HC=CH | 0.011 | 0.000 | 0.011 | 0.022 | 0.023 | −0.001 |
| Phenyl | 0.070 | 0.257 | −0.187 | 0.076 | 0.262 | −0.186 |
| $N(CH_3)_2$ | −0.002 | 0.182 | −0.184 | −0.002 | 0.175 | −0.177 |
| *cis*-DCM | | | | | | |
| Pyran cycle | 0.164 | −0.108 | 0.273 | 0.129 | −0.121 | 0.250 |
| $C(CN)_2$ | −0.240 | −0.337 | 0.097 | −0.222 | −0.357 | 0.135 |
| HC=CH | 0.032 | 0.012 | 0.020 | 0.041 | 0.025 | 0.016 |
| Phenyl | 0.055 | 0.268 | −0.213 | 0.063 | 0.267 | −0.194 |
| $N(CH_3)_2$ | −0.012 | 0.160 | −0.172 | −0.012 | 0.187 | −0.199 |
| *trans*-bis-DCM | | | | | | |
| Pyran cycle | 0.125 | −0.124 | 0.249 | 0.074 | −0.154 | 0.228 |
| $C(CN)_2$ | −0.289 | −0.362 | 0.073 | −0.246 | −0.361 | 0.115 |
| HC=CH | 0.038 | −0.001 | 0.039 | 0.050 | 0.020 | 0.030 |
| Phenyl | 0.088 | 0.270 | −0.182 | 0.104 | 0.291 | −0.187 |
| $N(CH_3)_2$ | 0.037 | 0.211 | −0.174 | 0.018 | 0.204 | −0.186 |
| *cis*-bis-DCM | | | | | | |
| Pyran cycle | 0.094 | −0.014 | 0.108 | 0.054 | −0.118 | 0.172 |
| $C(CN)_2$ | −0.285 | −0.216 | −0.069 | −0.269 | −0.373 | 0.104 |
| HC=CH | 0.076 | 0.051 | 0.025 | 0.084 | 0.052 | 0.032 |
| Phenyl | 0.083 | 0.107 | −0.024 | 0.096 | 0.234 | −0.138 |
| $N(CH_3)_2$ | 0.029 | 0.071 | −0.042 | 0.035 | 0.205 | −0.170 |

**Table 6.** MEP potentials $U$ (kJ mol$^{-1}$) for different conformations of DCM and bis-DCM molecules

| Molecule geometry | | $U$, kJ mol$^{-1}$ | | | |
|---|---|---|---|---|---|
| isomer | pyran cycle | $S_0$ | | $S_1$ | |
| | | N | O | N | O |
| DCM | | | | | |
| *Trans* | boat | −408 | −217 | −487 | −320 |
| | chair | −399 | −266 | −509 | −365 |
| *Cis* | boat | −389 | −237 | −448 | −446 |
| | chair | −395 | −235 | −469 | −420 |
| bis-DCM | | | | | |
| *Trans* | boat | −412 | −326 | −475 | −426 |
| | chair | −415 | −308 | −486 | −402 |
| *Cis* | boat | −391 | −295 | −456 | −432 |
| | chair | −396 | −288 | −460 | −412 |

increases on both centers (more significantly on the oxygen atom as compared with the nitrogen atoms of cyano groups).

The results obtained show that peculiar intermolecular interactions in DCM and bis-DCM molecules should arise even in the ground state and be enhanced in the $S_1(\pi\pi^*)$ state, while the solvatofluorochromic effect should be stronger than the solvatochromic effect; this is confirmed by the results of experimental study of the absorption and fluorescence spectra in different solvents [17, 26] and the increase in the dipole moment of molecules in the fluorescent state [10, 15, 16].

## CONCLUSIONS

Our study showed similarity of photoprocesses in DCM and bis-DCM molecules. The results of quantum-chemical calculations by the INDO method for

the energy and nature of electronic states correspond to the experimental data and allow one to interpret the deexcitation mechanisms for the excitation energy of molecules in low-polarity media. The method that we used allowed us to simulate the *trans–cis* photoisomerization. Rotation of molecules at close-to-right angles between the planes of pyran and phenyl cycles leads to a significant decrease in the energy of the $S_1$ state and an increase in the internal-conversion constant by several orders of magnitude. Thus, *trans–cis* photoisomerization explains the experimentally observed drop of the fluorescence quantum yield in nonpolar media.

Analysis of the electron density and MEP distributions in the ground and excited states allows one to explain the experimentally observed proton-acceptor properties of molecules—in particular, the stronger solvatofluorochromic (as compared with solvatochromic) effect—and confirms that there is efficient intramolecular transfer of electron density, which determines not only optical, but also conducting, properties of molecules and their application in optoelectronics.

## ACKNOWLEDGMENTS

This study was supported by grant no. NSh-13.05.2014.2 of the President of the Russian Federation and by the Ministry of Education and Science of the Russian Federation (task no. 2014/223 for the implementation of state works in the sphere of scientific activity, project code 1766).

## REFERENCES

1. Z. Y. Xie, L. S. Hung, and S. T. Lee, Appl. Phys. Lett. **79** (7), 1048 (2001).
2. A. Mukherjee, Appl. Phys. Lett. **62** (26), 3423 (1993).
3. S. Wang, Z. Bian, X. Xia, and C. Huang, Org. Electron. **11**, 1909 (2010).
4. Z. Abedi, M. Janghouri, E. Mohajerani, M. Alahbakhshi, A. Azari, and A. Fallahi, J. Lumin. **147**, 9 (2014).
5. A. M. Taleb, B. T. Chiad, and Z. S. Sadik, Renewable Energy **30**, 393 (2005).
6. B. Balaban, S. Doshay, M. Osborn, Y. Rodriguez, and S. A. Carter, J. Lumin. **146**, 256 (2014).
7. B. Wei, N. Kobayashi, M. Ichikawa, T. Koyama, and Y. Taniguchi, Opt. Expr. **14** (20), 9436 (2006).
8. X. Gu, L. Zhou, Y. Li, and Q. Sun, Phys. Lett. A **376**, 2595 (2012).
9. S. Popova, K. Pudzs, J. Latvels, and A. Vembris, Opt. Mater. **36**, 529 (2013).
10. C. R. Moylan, S. Ermer, S. M. Lovejoy, I.-H. McComb, D. S. Leung, R. Wortmann, P. Krdmer, and R. J. Twieg, J. Am. Chem. Soc. **118** (51), 12950 (1996).
11. M. Meyer, J.-C. Mialocq, and B. Perly, J. Phys. Chem. **94**, 98 (1990).
12. P. Meulen, H. Zang, A. M. Jonkman, and M. Glasbeek, J. Phys. Chem. **100**, 5367 (1996).
13. E. S. Voropai and M. P. Samtsov, Opt. Spectrosc. **82** (4), 534 (1997).
14. A. Maciejewski, R. Naskrwcki, M. Lorenc, M. Ziolek, J. Karolczak, J. Kubicki, M. Matysiak, and M. Skymanski, J. Mol. Struct., No. 555, 1 (2000).
15. Y. Zhou, Y. Liu, X. Zhao, and M. Jiang, J. Mol. Struct. (Theochem), No. 545, 61 (2001).
16. Y. Liu, Y. Liu, D. Zang, H. Hu, and C. Liu, J. Mol. Struct., No. 570, 43 (2001).
17. S. L. Bondarev, V. N. Knyukshto, V. I. Stepuro, A. P. Stupak, and A. A. Turban, Zh. Prikl. Spektrosk. **71** (2), 179 (2004).
18. V. A. Pomogaev, V. A. Svetlichnyi, A. V. Pomogaeva, N. N. Svetlichnaya, and T. N. Kopylova, Khim. Vys. Energ. **39** (6), 462 (2005).
19. Bo-C. Wang, H.-R. Liao, W.-H. Chen, Y.-M. Chou, J.-T. Yeh, and J.-C. Chang, J. Mol. Struct. (Theochem), No. 716, 19 (2005).
20. A. A. Turban, S. L. Bondarev, V. N. Knyukshto, and A. P. Stupak, Zh. Prikl. Spektrosk. **73** (5), 606 (2006).
21. A. V. Kulinich and A. A. Ishchenko, Usp. Khim. **78** (2), 151 (2009).
22. G. V. Maier, V. Ya. Artyukhov, O. K. Bazyl', T. N. Kopylova, R. T. Kuznetsova, N. R. Rib, and I. V. Sokolova, *Electronic Excited States and Photochemistry of Organic Compounds* (Nauka, Novosibirsk, 1997) [in Russian].
23. L. V. Levshin and A. M. Saletskii, *Optical Methods for Studying Molecular Systems. Part 1: Molecular Spectroscopy* (Izd-vo MGU, Moscow, 1994) [in Russian].
24. A. I. Kitaigorodskii, P. M. Zorkii, and V. K. Bel'skii, *Structure of Organic Materials (Data of 1971–1973)* (Nauka, Moscow, 1982) [in Russian].
25. R. S. Mulliken, J. Chem. Phys. **23** (10), 1833 (1955).
26. T. N. Kopylova, V. A. Svetlichnyi, L. G. Samsonova, N. N. Svetlichnaya, A. V. Reznichenko, O. V. Ponomareva, and I. V. Komlev, Kvantovaya Elektron. **33** (9), 807 (2003).
27. D. H. Waldeck, Chem. Rev. **91** (3), 415 (1991).
28. Breton. H. Le, B. Bennetau, J.-F. Letard, R. Lapouyade, and W. Rettig, J. Photochem. Photobiol. A **95** (1), 7 (1996).
29. N. G. Bakhshiev, *Spectroscopy of Intermolecular Interactions* (Nauka, Leningrad, 1972) [in Russian].

*Translated by Yu. Sin'kov*